Chemical Engineering Journal 166 (2011) 652–661

Contents lists available at ScienceDirect

Chemical Engineering Journal

journal homepage: www.elsevier.com/locate/cej

Evaluation of carbon-based materials in tubular biocathode microbial fuel cells in terms of hexavalent chromium reduction and electricity generation

Liping Huang[a,b,*], Xiaolei Chai[b], Shaoan Cheng[a,**], Guohua Chen[b,c]

[a] State Key Laboratory of Clean Energy Utilization, Department of Energy Engineering, Zhejiang University, Hangzhou 310027, China
[b] Key Laboratory of Industrial Ecology and Environmental Engineering, Ministry of Education (MOE), School of Environmental Science and Technology, Dalian University of Technology, Dalian 116024, China
[c] Department of Chemical and Biomolecular Engineering, The Hong Kong University of Science and Technology, Kowloon, Hong Kong, China

ARTICLE INFO

Article history:
Received 6 June 2010
Received in revised form 6 November 2010
Accepted 10 November 2010

Keywords:
Biocathode
Carbon-based material
Cr(VI) reduction
Microbial fuel cell
Tubular reactor

ABSTRACT

Biocathode microbial fuel cells (MFCs) are of great potentials in bioremediation of Cr(VI)-contaminant sites due to their low operating cost, self-regenerating ability and sustainable power supply. The improvement of Cr(VI) reduction rates and power generation, however, remains to be a challenging project. In the present study, graphite fibers, graphite felt and graphite granules were evaluated as biocatalytic cathode materials in tubular MFCs in terms of Cr(VI) reduction and electricity generation. At cathode to anode surface area ratio (C/A) of 3, graphite fiber was found superior to graphite felt or graphite granule. Specific Cr(VI) reduction rates ranging from 12.4 to 20.6 mg g^{-1} VSS h^{-1} and power generation from 6.8 to 15 W m^{-3} (20–48 A m^{-3}) were achieved in the biocatalytic graphite fiber cathode MFCs. Under a temperature of 22 °C and pH 7.0, Cr(VI) reduction followed pseudo-first-order kinetic model with the rate constant being $0.451 \pm 0.003\ h^{-1}$. In comparison with pH 7.0, an acidic pH of 5.0 improved Cr(VI) reduction of 27.3% and power generation of 61.8% whereas an alkaline pH of 8.0 decreased Cr(VI) reduction of 21.2% and power generation of 6.0%. It was found that the products formed whether as dissolved and/or precipitated Cr(III) was heavily pH dependent. Elevating temperature from 22 to 50 °C increased Cr(VI) reduction with the apparent activation energy (E_a) obtained as 10.6 kJ mol^{-1}. At high temperature of 50 °C, however, a decreased power generation was observed mainly because of the increase in anode potential. These results indicate that an optimal condition exists for efficient biocathode MFCs with quick Cr(VI) reduction and simultaneous high power generation.

1. Introduction

Hexavalent chromium is a priority toxic chemical normally present in wastewaters from electroplating, pigment, and lumber and wood product processes [1]. While physical and chemical methodologies can reduce Cr(VI) to Cr(III), a form of the metal with less toxicity, less solubility and less mobility [2,3], microbiologically catalyzed reduction is regarded as a safe and sustainable process for Cr(VI) wastewater treatment [4–7]. Slow Cr(VI) reduction rates, high-energy consumption and large amount of sludge production, however, are the main drawbacks of the conventional bioconversion process [8].

Microbial fuel cell (MFC) is a bioreactor that extracts energy from wastes and wastewaters through catalytic reactions of microorganisms [9]. Biocathode MFCs, which utilize electrochemically active microorganisms as catalysts at both cathode and anode, have attracted much attention. Various forms of MFCs have been tested which show great promise in bioremediation and waste treatment because their operations are inexpensive, catalysts self-regenerating and power supply sustainable [10–13]. Tandukar et al. reported recently that Cr(VI) can be reduced in a biocathode MFC, using a conventional H-type MFC configuration with graphite plate electrodes [14]. Their exploratory research opened the door for further investigation of maximizing reduction rate and bioelectricity generation as a function of reactor design, electrode character and system operation. For example, reducing the distance between the electrodes, using a composite electrode membrane assembly, enlarging the anode surface area, and optimizing MFC design in abiotic cathode MFCs would decrease the internal resistance by up to two orders of magnitude and increase the power density by 2–3 orders of magnitude [15–20]. In contrast, the enlargement of the air biocathode MFC reactor by a factor of 2.9–3.8 reduced the vol-

* Corresponding author at: State Key Laboratory of Clean Energy Utilization, Department of Energy Engineering, Zhejiang University, Hangzhou 310027, China. Tel.: +86 571 87952038; fax: +86 571 87951616.
** Corresponding author. Tel.: +86 571 87952038; fax: +86 571 87951616.
E-mail addresses: lphuang2008@gmail.com (L. Huang), shaoancheng@zju.edu.cn (S. Cheng).

1385-8947/$ – see front matter © 2010 Elsevier B.V. All rights reserved.
doi:10.1016/j.cej.2010.11.042

umetric power output by 60–67% [21]. Similarly, a comparatively low power production was suspected for a large biocathode reactor [22]. Although a large surface area ratio of cathode (graphite granule) to anode (graphite plate) of around 100–280 in a biocathode H-type MFC showed an improved system performance, the Cr(VI) reduction rate obtained was still lower than that of the conventional aerobic and anaerobic processes [8,23]. Obviously, there are more work to be done to improve the Cr(VI) reduction rate on the biocathode in order to maximize the advantages of biocathode MFCs over conventional biological processes and realize the potentials of biocathode MFCs for Cr(VI) reduction.

The tubular or two-cylinder shape MFC has advantages over the H-type MFC because of the reduced electrodes spacing and the large proton exchange area, both of which lead to a lower internal resistance and therefore an improved system performance [21,24,25]. Carbon-based packing materials such as graphite fibers, graphite felt and graphite granules were often employed as biocathodes for high power generation and efficient nitrate or oxygen reduction because of their high specific surface area [21,25–27]. Thus, an integrated system of packing carbon-based materials inside a tubular MFC may be a technically sound approach to improve the electricity generation and Cr(VI) reduction rates in biocathode MFCs. Moreover, pH [18,26,27,31,34] and temperature [28–30,32,33] have been reported to affect the performance of abiotic cathode or biocathode using nitrate or oxygen as an electron acceptor, they are expected to influence the performance of biocathode MFCs system using Cr(VI) as a terminal electron acceptor. In this study, therefore, we firstly tested Cr(VI) reduction and power generation in tubular biocathode MFCs with three different carbon-based packing materials namely graphite fibers, graphite felt and graphite granules. Graphite fibers were then used to investigate the effects of cathode to anode surface area ratios (C/A) on Cr(VI) reduction and electricity generation while effects of temperature and pH were also assessed and discussed. Interesting results have been found as discussed subsequently.

2. Materials and methods

2.1. MFC construction

The tubular MFC was similar to the one reported by Clauwaert et al. [25]. The cathode chamber was a 7.0 cm (inner diameter) × 6.4 cm high cylindrical Plexiglas (2-mm thick). A cylindrical cation exchange membrane (CEM) (CMI-7000 Membranes International, Glen Rock, NJ) (4.0 cm in diameter and 6.4 cm in height) was centrally located inside, forming an outer cathode chamber and an inner anode chamber (Fig. 1). The cathodic and anodic volumes were 160 and 80 mL, respectively. Both the cylindrical cathode and anode were tightly bonded to the Plexiglas base (7.0 cm in diameter) and sealed with superglue. The reactor was capped with a same size Plexiglas disk with holes for anode electrodes, cathode electrodes, reference electrodes and external circuit wires. Graphite fibers [15] were used as anode in all of the reactors. Various carbon-based materials including graphite fibers, graphite granules and graphite felt (Sanye Co., Beijing, China) were firstly packed in the cathode chamber to achieve a ratio of cathode to anode surface areas (C/A) of 3:1 to investigate the effects of cathode materials on power generation and Cr(VI) reduction rate. The specific surface areas of these porous industrial grade materials were estimated to be 800 $m^2\ m^{-3}$ for graphite granules, 2000 $m^2\ m^{-3}$ for graphite felt and 9600 $m^2\ m^{-3}$ for graphite fibers, respectively. The cathodic working volume was 85 mL. Before the installation, these materials were treated in the same way as reported by Clauwaert et al. [25]. A reference electrode (Ag/AgCl electrode, 195 mV versus standard hydrogen electrode, SHE) was used to obtain cathode and anode potentials. Two duplicate reactors were operated as controls: one is used for the exclusion of biological catalysis of Cr(VI) reduction (abiotic control), the other control was run in the open circuit mode (disconnected electrode) for Cr(VI) reduction (anaerobic control). All of the reactors were wrapped with aluminium foil to avoid the photo illumination.

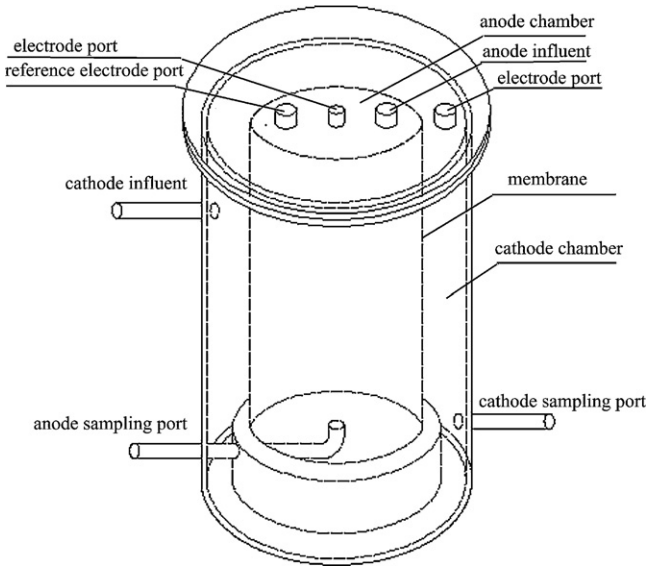

Fig. 1. Diagram of tubular reactor.

2.2. Inoculation and operation

The cathode in the present MFC was inoculated with a mixed bacterial culture obtained from an MFC that had been operating for more than 6 months using Cr(VI) as an electron acceptor in cathode chamber. An acclimated mature anode made of graphite fibers was directly transferred from the anode chamber of the previous reactor for similar research [35] and used as anode in this study. The medium composition in both cathode and anode chambers were the same as previously reported [23]. The reactor was run in fed-batch mode at temperature of $22 \pm 2\ ^\circ C$ except the cases where temperature effects were examined at 35 and 50 °C, respectively. In the investigation of pH effects, initial anolyte was always kept at pH 7.0 while the feed solution in cathode was adjusted by weak acid or base solution to the desired values. The concentration of phosphate buffer remained the same at different pH values.

2.3. Analyses and calculations

The voltage across an external resistor was continuously recorded using a data acquisition system. Current, power and Coulombic efficiencies (CEs) were calculated as previously described [22]. A commonly used method termed as linear sweep voltammetry (LSV) was employed here for the determination of maximum power density [36,37]. Based on previously reports [25,27], a scan rate of 1 $mV\ s^{-1}$ was firstly chosen to obtain the polarization curves in fiber-3 reactors. Another method termed as "multiple cycles" was then used for comparison in order to evaluate the reliability of 1 $mV\ s^{-1}$ for the present study. For the "multiple cycles" method, a single cycle was run for each resistor. The maximum power density value was taken at steady state conditions. When the current started to decrease, the solution was replaced before using a new resistor.

Samples were withdrawn as appropriate using a syringe. They were centrifuged immediately. The supernatants were analyzed

right after the centrifugation for residual soluble Cr(VI) and total soluble chromium using a colorimetric standard method [38]. The amount of dissolved Cr(III) was calculated as the difference between the concentration of the total soluble chromium and that of hexavalent chromium. Biomass in the cathode chamber was measured according to the standard method [38]. All measurements were taken over two or three consecutive retention times. The bacterial morphologies on different graphite-based electrodes were observed using a scanning electron microscope (SEM; Hitachi, S570, Japan). Prior to observation, these carbon-based materials were collected and fixed overnight with paraformaldehyde and glutaraldehyde in buffer solution (0.1 M cacodylate, pH 7.5, 4 °C), followed by washing and dehydration in water/ethanol solutions. Samples were then coated with Au/Pt before SEM observation.

3. Results and discussion

3.1. Electricity generation during start-up

After a lag period of 50–58 h after first inoculation, there was an increase in voltage output in all of the reactors with different cathodes, reaching 0.31–0.36 V across a fixed resistor of 1000 Ω. Power was generated at the start of the second fed-batch cycle. After the fifth cycle, the electricity cycles became consistent and reproducible exhibiting voltage around 0.45–0.52 V with the anode potential being stably around −0.30 V during the experimental periods. These results demonstrate that the increase in voltage output was mainly attributed to the improved performance of cathodes, on which stably and electrochemically active biofilms had been formed (data not shown).

3.2. Time course of electricity generation and Cr(VI) reduction in biocatalytic carbon-based cathode MFCs

Fig. 2 shows the influence of different carbon-based materials on the performance of biocathode MFCs. For all the three materials tested, the electric current increased with time initially and dropped towards the end of the experiment resulting in a peak value shortly after 1 h operation (Fig. 2A). Comparatively, granule-3 produced a low power of 7.6 A m^{-3} (2.0 W m^{-3}) whereas power produced from felt-3 and fiber-3 reached 10.5 A m^{-3} (3.8 W m^{-3}) and 11.5 A m^{-3} (4.5 W m^{-3}), respectively, indicating no great difference of power generation between fiber-3 and felt-3. In the abiotic controls, only 1.7 A m^{-3} (0.1 W m^{-3}) was obtained, showing the importance of electrochemically active microorganisms on electricity generation.

Along with the electricity generation, Cr(VI) concentration in biocathode MFCs decreased gradually as expected (Fig. 2B). Fiber-3 cathode gave a higher Cr(VI) reduction rate of 3.61 ± 0.10 mg L^{-1} h^{-1} than that of the felt-3 (3.07 ± 0.12 mg L^{-1} h^{-1}) or the granule-3 (3.46 ± 0.09 mg L^{-1} h^{-1}). Considering the biomass in the three biocathode chambers, which was around 0.28–0.37 g L^{-1} for fiber-3, 0.30–0.35 g L^{-1} for felt-3, and 0.57–0.67 g L^{-1} for granule-3, respectively, the specific Cr(VI) reduction rate was therefore 11.3 ± 2.2 mg g^{-1} VSS h^{-1} for fiber-3, 9.5 ± 1.0 mg g^{-1} VSS h^{-1} for felt-3, and 5.6 ± 0.6 mg g^{-1} VSS h^{-1} for granule-3.

3.3. SEM characterization on carbon-based materials with or without a biofilm

The difference in the nature of the electrode materials is illustrated in Fig. 3 by the scanning electron microscopy images of carbon-based materials before and after biofilm formation (120 days of operation). Generally speaking, sparse coverage of bacteria was found on these carbon-based electrodes (Fig. 3B, D, and F), which was similar to the biocathodes using oxygen or carbon dioxide as terminal electron acceptors [39,40]. In comparison with graphite granule (Fig. 3E and F), there is more space between intersectional graphite fiber and graphite felt (Fig. 3A–D). This kind of porous structure may allow for better substrate access resulting in a higher current density in graphite fibers and graphite felt than graphite granules [15,19]. In addition, more perpendicular positioned bacteria on the graphite fibers were observed (Fig. 3B) while bacteria on graphite felt were mostly attached (Fig. 3D). These bacterial morphologies on the cathode were similar with the reported [39,40].

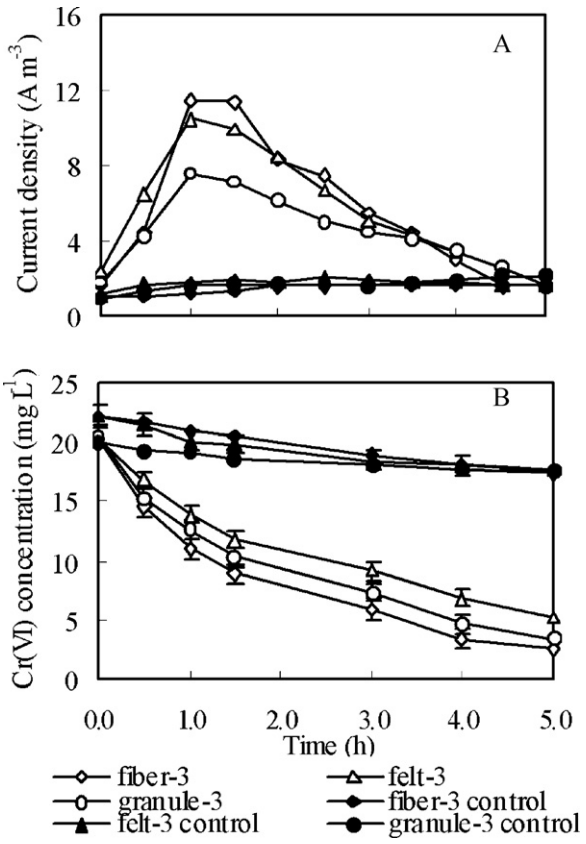

Fig. 2. Electricity generation (A) and Cr(VI) concentration (B) as a function of incubation time in biocatalyzed carbon-based cathode MFCs (external resistor: R_{ex} = 400 Ω).

The findings here are consistent with the results reported by You et al. who found the biocatalytic graphite fiber cathodes produced higher power than graphite granule cathodes [27]. In terms of power generation, the performance of biocathode can be affected by multiple factors such as electrode electrical conductivity, bacterial accessibility, mass transfer, and surface morphology of electrode material [12]. The efficient mass transfer in graphite fiber and graphite felt system offers one possible reason for the observed results [15,27]. Other factors, such as surface roughness of cathode electrode, the properties of attached biofilm, and the level of electrode potential, may also contribute to the noted current generation although there is not a generally agreed relationship [12,40–48]. The increase in polishing level decreased the surface roughness value and the amount of bacterial adhesion, while a rough surface promoted bacterial adhesion and colonization, and high-energy surfaces collected more bacteria, bound the bacteria more strongly, and selected for specific bacteria [42–44]. However, a smoother initial surface of glassy carbon electrode and stainless steel electrode can lead to the growth of a more compact and homogeneous biofilm of *Leptothrix discophora* SP-6 [45]. Also, a

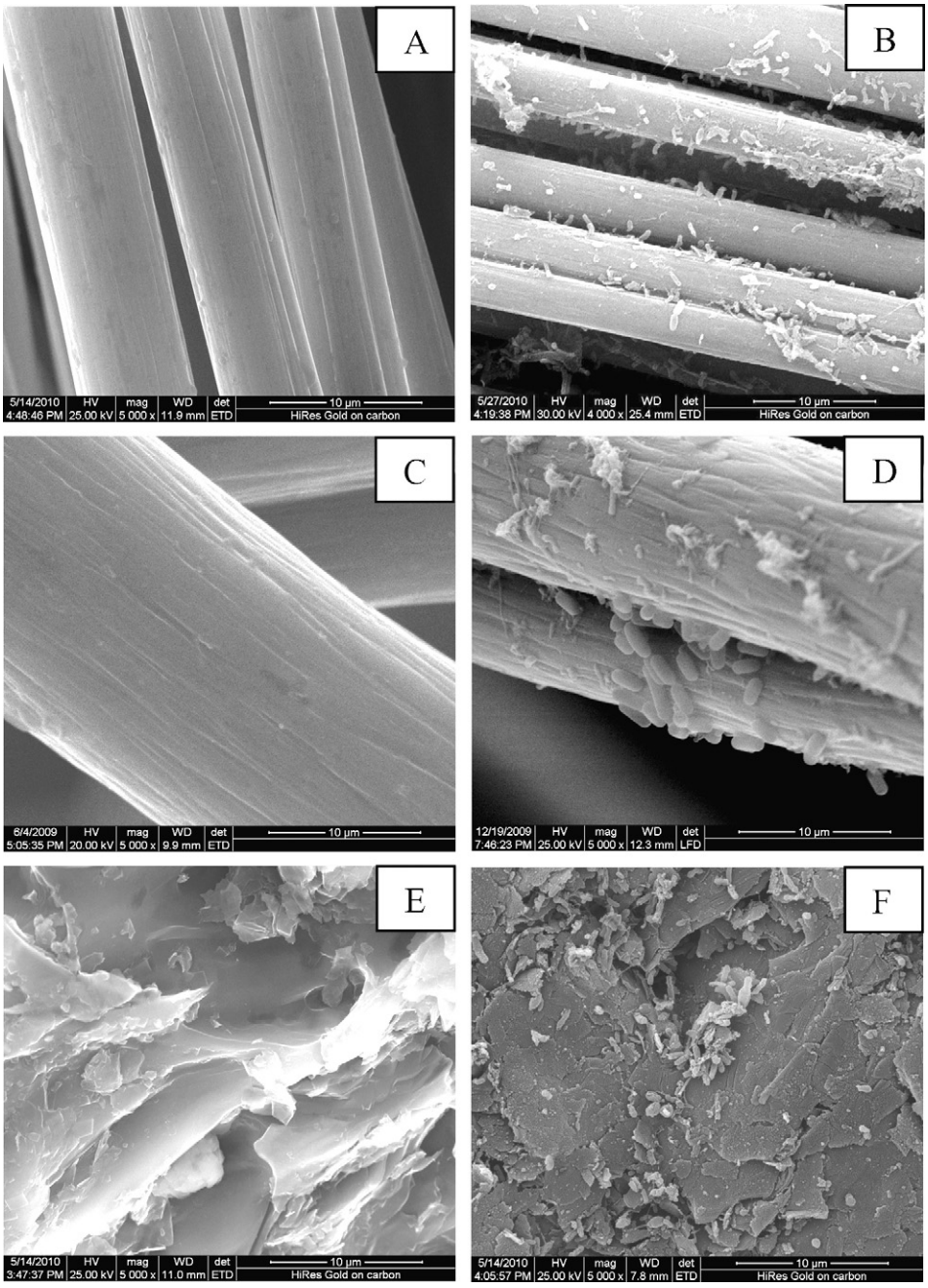

Fig. 3. Scanning electron micrographs on different carbon-based materials before and after biofilm formation. (A) graphite fiber without biofilm, (B) graphite fiber with biofilm attached, (C) graphite felt without biofilm, (D) graphite felt with biofilm attached, (E) graphite granule without biofilm, and (F) graphite granule with biofilm attached.

stainless steel biocathode provided 25 times higher power density than graphite under identical conditions and showed excellent electrokinetic properties to support fumarate reduction catalyzed by pure culture of *Geobacter sulfurreducens* [46]. On the other hand, in terms of Cr(VI) reduction, a higher specific Cr(VI) reduction rate in graphite fibers than graphite felt and graphite granules may be attributed to the more efficient biocatalytic activity, showing with a less biomass production and a quicker decrease of Cr(VI) concentration in per catholyte volume and per hour in graphite fiber chamber. This result was consistent with other researchers' report that thinner biocatalytic films on the cathode corresponded with better system performance [48]. Therefore, further exploration should be focused on the relationships among graphite fiber electrode roughness, electrode electrical conductivity, biofilm thickness and microbial consortia composition or specific bacteria, and system performance of Cr(VI) reduction and electricity generation. However, it is beyond the scope of the present study. In the following experiments, graphite fibers were chosen as cathode for further investigations.

3.4. Effect of ratios of C/A in biocatalytic graphite fiber-cathode MFCs

The two polarization methods, namely LSV and multiple cycle methods, were firstly compared in the evaluation of maximum power. The average maximum power density produced using multiple cycle method was of $6.3 \pm 0.2\,W\,m^{-3}$ at a current density of $19\,A\,m^{-3}$ while that obtained using LSV was $6.8 \pm 0.1\,W\,m^{-3}$ at a current density of $20\,A\,m^{-3}$ (Fig. 4A and B), illustrating no significant differences between the two methods for the present study.

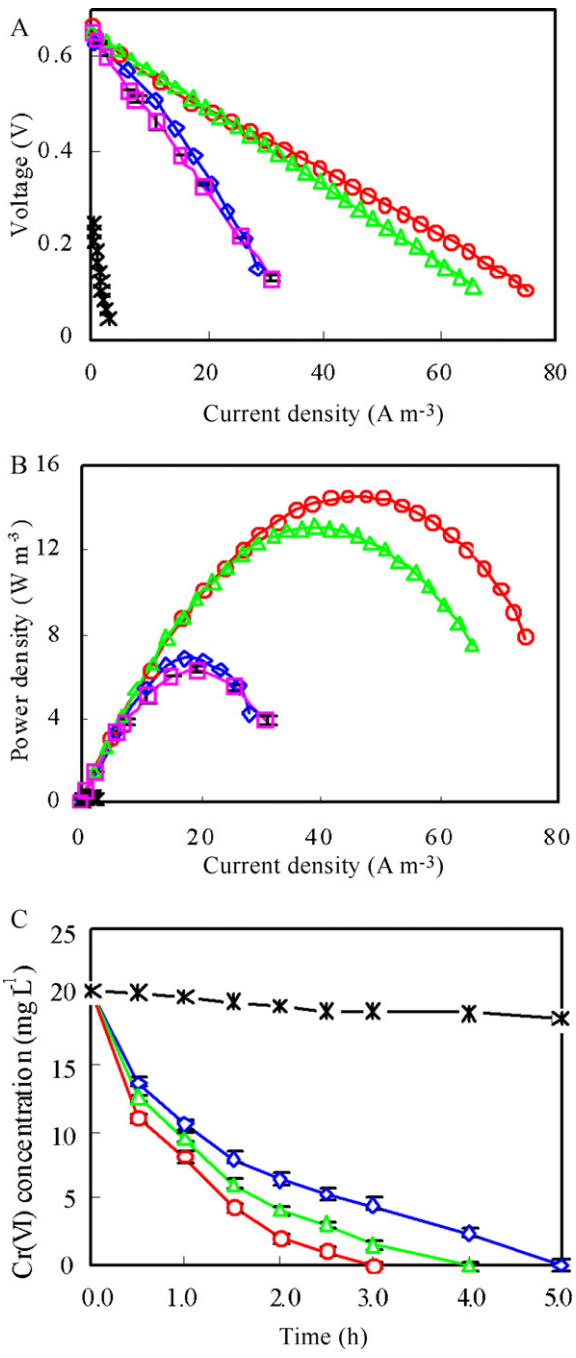

Fig. 4. Polarization (A), power density (B) curves and time course of Cr(VI) reduction (C) in biocatalyzed graphite fiber-cathode MFCs with different ratios of C/A (◊: fiber-3, Δ: fiber-10, ○: fiber-20, *: open circuit control). In the case of Cr(VI) reduction, R_{ex} was set at 200 Ω for fiber-3, 100 Ω for fiber-10 and 80 Ω for fiber-20, respectively. Comparison of power density outputs using different polarization methods (□: multiple cycles, ◊: LSV) was also shown in (A) and (B) (initial pH: 7.0, operation temperature: 22 °C).

LSV method was therefore used for maximum power in the following investigations. This result may also indicate that the bacteria on the current biocathode exhibited a quicker response to the changes of voltage at a rate of 1 mV s^{-1} than that reported by others previously [25,37].

Different ratios of C/A such as 20 (fiber-20), 10 (fiber-10) and 3 (fiber-3) were respectively set to investigate the effects of cathode surface area on power generation and Cr(VI) reduction in the current biocathode MFCs. There were slight increases in open circuit potential (OCP) with the increase in electrode surface area ranging from 0.63 V at fiber-3 to 0.67 V at fiber-20 (Fig. 4A). In the control (abiotic cathode, pH of 7.0 and temperature of 22 °C were the same as biotic system) with fiber-3 electrode, OCP of 0.24 V was much lower than the 0.63–0.67 V, confirming that the involved microorganisms significantly enhanced the OCP of the present system. Greatly different from a quicker change of voltage with current density at fiber-3, fiber-10 and fiber-20 showed a comparatively slow voltage decrease with current density, illustrating a lower internal resistance in the biocatalytic larger surface area cathode systems. The larger surface area corresponded with more biocatalyst reaction sites and may permit quicker electron exchange around cell surface, especially under the condition of higher current density, and consequently resulted in less voltage losses with current density course. The internal resistances calculated from the polarization curves were 82, 96 and 231 Ω for fiber-20, fiber-10 and fiber-3, respectively.

The maximum power values generated by the three biocatalytic graphite fiber cathode MFCs are 15 W m^{-3} at 48 A m^{-3} for fiber-20, 13 W m^{-3} at 39 A m^{-3} for fiber-10, and 6.8 W m^{-3} at 20 A m^{-3} for fiber-3, substantially higher than the 0.19 W m^{-3} at 1.9 A m^{-3} for abiotic cathode (Fig. 4B). In comparison with the 0.13 W m^{-3} in graphite plate cathode and 1.3 W m^{-3} in graphite granule cathode [14,23], the power densities of this biocathode were therefore 53–117 times that of graphite plate and 5.2–12 times of graphite granules, respectively at the same concentration of Cr(VI) in a biocathode H-type MFCs. CEs obtained from the graphite fiber MFCs were around 98–100%, higher than the 78% in the biocatalytic graphite granule cathode and H-type MFCs [23], demonstrating the high utilization efficiency of electrons transferred from anode in the present tubular biocathode system. The increase in cathode surface area increased the quantity of catalystic bacteria on the cathode and thereby improved the performance of the MFC system by decreasing the activation overpotential of the biocathode electrode, leading to the increase in cathode potential and power production [12,19]. Similar observation of an increase in power due to a reduction in cathode overpotential was also made using biocathodes with oxygen and nitrate electron acceptors [25,26,34].

Under the optimized external resistances, Cr(VI) reduction rate in fiber-3, fiber-10 and fiber-20 reached 4.08, 5.12 and 6.80 mg L^{-1} h^{-1}, respectively (Fig. 4C). Accordingly, based on the biomass in the biocathode system, which was around 0.28–0.37 g L^{-1}, the specific Cr(VI) reduction rates on the graphite fiber cathodes were therefore 12.4–20.6 mg g^{-1} VSS h^{-1}, respectively. These values were 69–114 times and 6.2–10.3 times, respectively, as high as the previously reported using the same electron acceptor and a bio-catalyzed carbon plate or graphite granule cathode H-type MFCs, showing the importance of coordinated effects of cathode surface area and reactor architecture on the biocathode performance [12,23]. Additionally, the values obtained here are 3.6–6.1 times and 3.3–5.6 times, respectively, as high as the highest Cr(VI) reduction rates recently reported in conventional aerobic and anaerobic Cr(VI) reduction processes [8].

Electrode surface area is one important factor for reactor performance. Increasing cathode surface area and retaining a small anode relative to the cathode area has been suggested extensively to keep abiotic cathodic reactions from limiting rates of electron transfer at the bioanode and therefore to improve power production [12,19]. In the case of biocathode systems, more cathode surface area can increase the quantity of catalyst bacteria on the surface and thereby provide more available reaction sites for cathodic reactions in an identical cathode compartment [23,27]. On the other hand, a comparatively small surface area of membrane between a two-chamber MFC and a relatively long average distance between anode and cathode increases the resistance associated with the membrane and electrolyte, and consequently increases the internal resistance of the system [12,48,49]. In the case of a small size

membrane (4.9 cm^2), a long average distance between anode and cathode (12.5 cm) and over-enlargement of the cathode surface area (e.g. ratio of C/A was around 100–280) in a typical H-type biocathode MFC, membrane resistance and electrolyte resistance may have heavily limited the system performance [23]. Comparatively, the present tubular MFC equipped with a large size membrane (80.4 cm^2), a short average distance between anode and cathode (1.75 cm), and ratios of C/A of around 3–20 may have efficiently improved mass transfer and decreased internal resistance, which resulted in a better system performance than the previous one [23]. These results were consistent with other observations, which demonstrated cathode surface area and reactor architecture were limiting the performance of biocathode MFCs using oxygen or nitrate as a terminal electron acceptor [21,27].

3.5. Effect of initial Cr(VI) concentrations

OCP increased with the increase in initial Cr(VI) concentrations from 0.63 V at 20 mg L^{-1} to 0.66 V at 40 mg L^{-1}, Fig. 5A, demonstrating the decrease in activation losses with the increase in Cr(VI) concentrations at this range [14]. This result can be also explained by Eq. (1), in which a high Cr(VI) concentration pushes the reaction of Cr(VI) reduction forward in a positive direction. Further increase in the initial Cr(VI) concentration to 50 mg L^{-1} resulted in an apparent decrease of OCP to 0.57 V, illustrating the inhibitory effect of this higher Cr(VI) concentration on the catalytic activity of electrochemical bacteria. In the abiotic control (pH of 7.0 and 22 °C, the same conditions as biotic system), OCP was only around 0.24 V, showing the importance of biocatalysts on the increase of OCP in the present biocathode system. A maximum power of 7.2 W m^{-3} at a current density of 19 A m^{-3} was obtained at 40 mg L^{-1} while it was only 4.1 W m^{-3} at a current density of 13 A m^{-3} for an initial Cr(VI) concentration of 50 mg L^{-1} (Fig. 5B).

$$Cr_2O_7^{2-} + 14H^+ + 6e^- \rightarrow 2Cr^{3+} + 7H_2O \quad (1)$$

$$2Cr^{3+} + 7H_2O \rightarrow 2Cr(OH)_3(s) + 6H^+ + H_2O (6.5 < pH < 10) \quad (2)$$

Data from kinetic experiments with varying initial Cr(VI) concentrations and optimized external resistances were collected to investigate the reaction orders. For each experiment within 3 h reaction time, reaction rates were well described by a pseudo-first-order model of the form:

$$\ln \frac{C_0}{C} = k_{obs} \times t \quad (3)$$

where k_{obs}, pseudo-first-order rate constant (h^{-1}); C_0, initial Cr(VI) concentration (mg L^{-1}); and C, dissolved Cr(VI) concentration at time t (mg L^{-1}); t, running time (h).

Good fits ($R^2 > 0.974$) of all experimental data were obtained using the pseudo-first-order model. The slope of $\ln(C_0/C)$ versus time was equal to the rate constant k_{obs}. As shown in Fig. 5C, this value (mean $k_{obs} = 0.451 \pm 0.003\ h^{-1}$, $n = 4$) was essentially constant over the range of C_0 from 20 to 40 mg L^{-1}, indicating the suitability of the pseudo-first-order model for the present biocathode system. In the case of 50 mg L^{-1} Cr(VI), however, inhibitory action of Cr(VI) on the electrochemically active biofilm may have happened, shown an apparent decrease in cathode potentials from 0.03 V at 20 mg L^{-1} to −0.05 V at 50 mg L^{-1} ($R_{ex} = 200\ \Omega$). The specific Cr(VI) reduction rates at 50 mg L^{-1} was only around 5.2 mg g^{-1} VSS h^{-1} and therefore resulted in the disagreement with the pseudo-first-order model.

3.6. Effect of initial pHs

A set of experiments were performed at different cathode initial pHs ranging from 5.0 to 8.0 to investigate the effect of pHs on Cr(VI) reduction and power generation as shown in Fig. 6. Open circuit potential exhibited difference at various pH values ranging from 0.54 V at pH 8.0 to 0.76 V at pH 5.0 (Fig. 6A). The maximum power density increased with decreasing pH and reached the highest value of 11 W m^{-3} at a current density of 24 A m^{-3} and pH 5.0 while it was only around 6.4 W m^{-3} at a current density of 20 A m^{-3} and pH 8.0, an improvement of 61.8% and a decrease of 6.0%, respectively compared to the value of 6.8 W m^{-3} at pH 7.0 (Fig. 6B). In comparison with anode potentials which was stable around −0.30 V, cathode potentials increased from 0.03 V at pH 8.0 to 0.13 V at pH

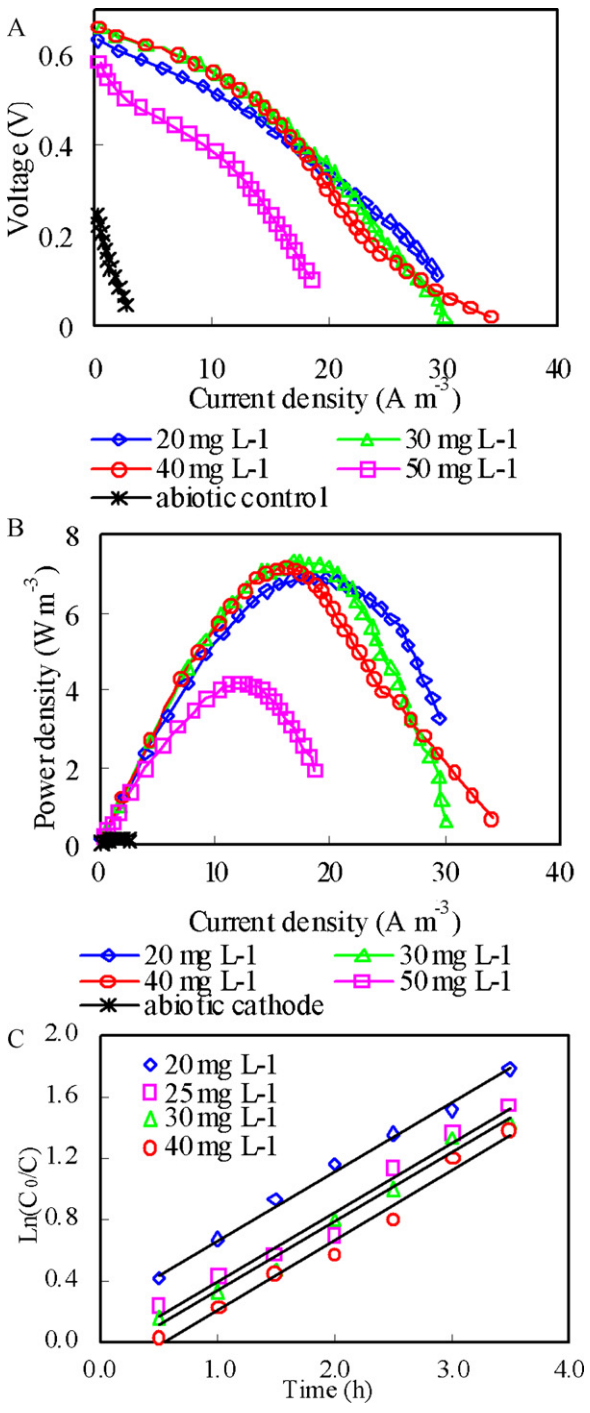

Fig. 5. Polarization (A), power density (B) and time course of dissolved Cr(VI) (indicated as $\ln(C_0/C)$) (C) under various initial Cr(VI) concentrations in biocatalyzed fiber-3 cathode MFCs (pH: 7.0, temperature: 22 °C).

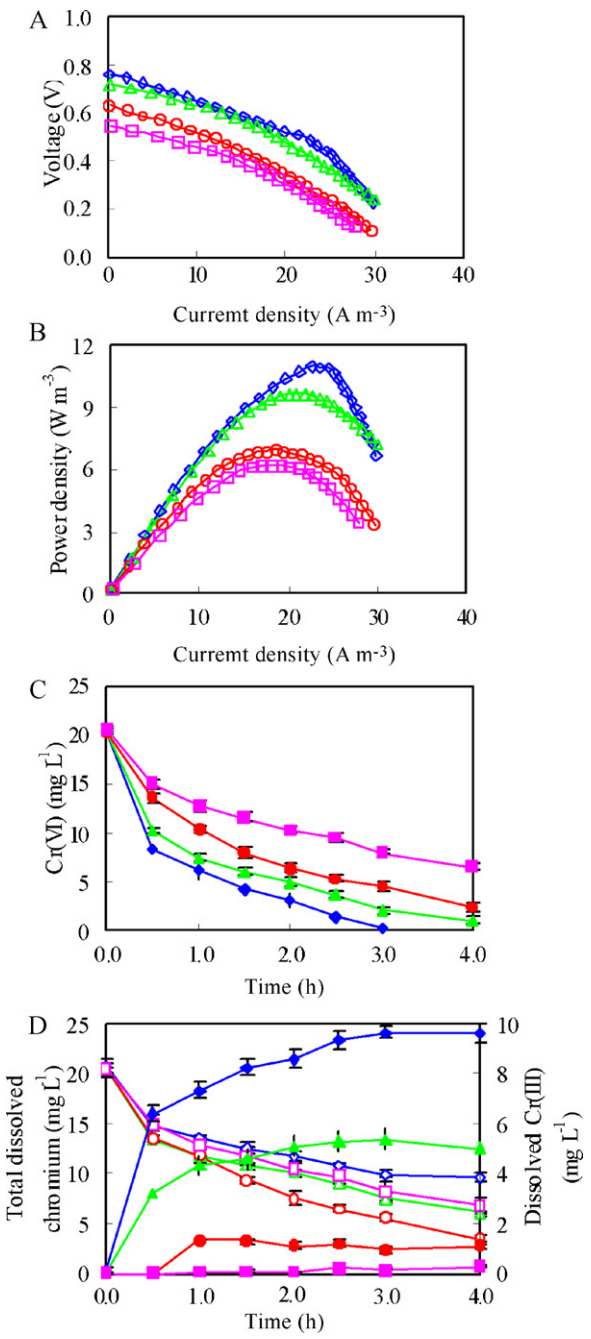

Fig. 6. Voltage (A) and power density (B) as a function of external resistance, and time courses of dissolved Cr(VI) (C), total chromium (D, open symbol) and dissolved Cr(III) (D, solid symbol) at pH 5.0 (diamond), 6.0 (triangle), 7.0 (circle) and 8.0 (square) in biocatalyzed fiber-3 cathode MFCs (temperature: 22 °C, initial Cr(VI) concentration: 20 mg L^{-1}).

5.0 (R_{ex} = 200 Ω), illustrating power increase was attributed to the improvement of biocathodes.

Electrode potentials at 298 K exhibit a function of pH values according to Nernst equation as described in Eq. (4) [50]. A theoretically net change of potential with pH change was therefore shown in Eq. (5). Decrease in three pH units theoretically reduced potential of 0.177 V (Eq. (5)). In the case of the present biocathode system, a decrease of cathode pH actually increased cell potential from 0.54 V at pH 8.0 to 0.76 V at pH 5.0 (Fig. 6A), indicating a net potential increase of 0.22 V. This value was even higher than the theoretical value of 0.177 V resulted from abiotical decrease of 3 pH units, indicating a positive response of catalysis activity of electrochemical microorganisms to pH decrease.

$$E = E_0 - 0.0591\text{pH} \quad (4)$$

$$\Delta E = 0.0591\ \Delta\text{pH} \quad (5)$$

Concurrently with electricity generation, a decrease in the pH of the biocathode electrolyte resulted in an increase in the rate of Cr(VI) reduction (Fig. 6C) and the formation of dissolved Cr(III) (Fig. 6D). Within a period of 3 h, around 98.5% Cr(VI) was reduced at pH 5.0, whereas 61.0% Cr(VI) reduction was observed at pH 8.0, 61.6% increase of Cr(VI) reduction with a decrease of pH from 8.0 to 5.0 (Fig. 6C). In the abiotical control, systems at pH 5.0 and pH 8.0 exhibited Cr(VI) reduction of 11.2% and 7.3%, respectively, illustrating the more efficient Cr(VI) reduction in biocathode system at pH 5.0 than pH 8.0 was mainly due to microbial catalysis and not abiotical mediation. Higher product of dissolved Cr(III) was observed in solution at pH 5.0 compared to pH 8.0 (Fig. 6D). At pH 5.0, dissolved Cr(III) was increased to 8.6 mg L^{-1} within the first 2 h of the experiment and kept around 9.3 mg L^{-1} during the following running period. At pH 8.0, however, no more than 0.3 mg L^{-1} of dissolved Cr(III) was observed over the duration of the time course. While total dissolved chromium at various initial pHs decreased with the time course, pH 5.0 followed by pH 8.0 had higher total dissolved chromium than pH 6.0 and 7.0, indicating more acidic or alkaline condition was beneficial to the formation of dissolved chromium (Fig. 6D). However, at pH 5.0, the total dissolved chromium was mainly composed of dissolved Cr(III) while at pH 8.0, it was mainly attributed to the dissolved Cr(VI) (Fig. 6D).

The complex biological and electrochemical reactions in the biocathode system can be heavily affected by pHs. On the one hand, pHs can affect the surface properties of the cells including cell surface hydrophobicity, net surface electrostatic charge, cell surface shape and polymers, cell morphology, cell size at cell division, time to division as well as biofilm structure [51,52], and consequently affect the bio-catalytic activity on electron transfer from cathode to bacteria and Cr(VI) reduction inside cells or extracellularly. On the other hand and in terms of chemical reactions, the net Cr(VI) reduction theoretically consumes protons on the basis of Eqs. (1) and (2). Rates of Cr(VI) reduction by various organic reductants increased with decreasing pHs owing to the increased protonation level of Cr(VI) species [53,54]. In the case of the present biocathode system, a similar speciation effect at a lower pH of 5.0 may therefore be beneficial for not only the catalysis activity of electrochemical microorganisms, but also Cr(VI) reduction via chemical and biological reactions. Our result was similar to the those previous reported by Virdis et al. [26] and Clauwaert et al. [34], in which an acidified cathode influence or an appropriate pH neutralizing action can enhance the bio-catalytic activity for de-nitrification process, during which alkalinity was produced.

3.7. *Effect of temperature*

Lower ambient temperatures are more relevant for wastewater treatment applications. Additionally, the seasonal temperature change is a practical condition to adopt. It is therefore essential to investigate the temperature effects on system performance. Meanwhile, temperature may be regulated to not only accelerate chemical reaction rate, but also keep high biocatalyst activity, both of which will improve system performance [28–30,32,33]. Based on these considerations, three temperature levels namely 22, 35 and 50 °C were investigated in the present study. Open circuit potential slightly increase with the increase in temperature from 0.63 V at 22 °C to 0.68 V at 35 °C while voltage output at higher current densities (>10 A m^{-3}) became more apparently affected during this temperature range (Fig. 7A). Further increase in temperature to

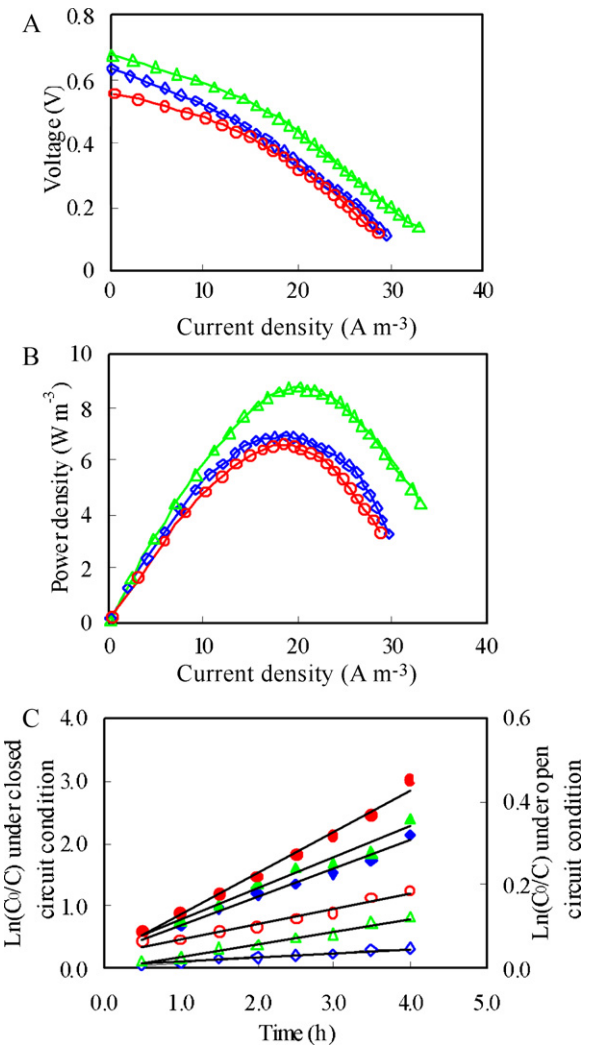

Fig. 7. Voltage (A) and power density (B) as a function of external resistance, and time course of dissolved Cr(VI) (shown as $\ln(C_0/C)$) under closed circuit (solid symbol) or open circuit (open symbol) conditions (C) at temperatures of 22 °C (diamond), 35 °C (triangle) and 50 °C (circle) (pH: 7.0, initial Cr(VI) concentration: 20 mg L^{-1}).

50 °C led to apparent decrease in open circuit potential (0.56 V) and voltage output (Fig. 7A).

Along with the voltage output, maximum power density increased with temperature from 6.8 W m^{-3} at 22 °C to 8.7 W m^{-3} at 35 °C, a 28% improvement within the temperature range (Fig. 7B). Further increase in temperature to 50 °C lowered open circuit potential (Fig. 7A) and decreased the maximum power density to 6.6 W m^{-3} (Fig. 7B).

Potentials of anode and cathode exhibited different change with the increase of temperature. At a fixed external resistance of 200 Ω, anode potentials changed little at a temperature range of 22–35 °C while cathode potentials increased from 0.03 V at 22 °C to 0.07 V at 35 °C, mainly contributing to the increase in power from the system at this temperature range. Further increasing temperature from 35 to 50 °C increased cathode potential from 0.07 V to 0.10 V, and anode potential from −0.30 V to −0.235 V, resulting in a net decrease in voltage output from 0.37 V to 0.335 V. Thus, the lower electricity generation at a high temperature of 50 °C was mainly attributed to the decrease in the activity of electrochemical biofilm on the anode.

Similar to the kinetic effects at different initial Cr(VI) concentrations, data with varying temperatures under closed circuit and open circuit conditions were collected. For each temperature, reaction rates were well described by a pseudo-first-order model. The k_{obs} obtained increased from 0.457 h^{-1} to 0.663 h^{-1} with the increase in temperature from 22 to 50 °C (Fig. 7C).

$$\ln K_{obs} = \ln K_0 - \frac{E_a}{RT} \quad (6)$$

According to Arrhenius equation (Eq. (6)) and the k_{obs} obtained under different temperatures, $1/(RT)$ versus $\ln k_{obs}$ was plotted, and the apparent activation energy (E_a) can be found from the slope of the straight line. The calculated E_a values were 10.6 kJ mol^{-1} for closed circuit condition and 32.3 kJ mol^{-1} for open circuit condition, respectively. The E_a of 32.3 kJ mol^{-1} under the open circuit condition was similar to the 33 and 46 kJ mol^{-1}, obtained from chemical reaction processes, and higher than the 21 kJ mol^{-1}, a minimum value for estimating chemically controlled processes [2,3]. Thus, Cr(VI) reduction under the present open circuit condition was chemical reaction controlled. However, the E_a of 10.6 kJ mol^{-1} obtained under the closed circuit (biocatalysis) condition was much lower than the 21 kg mol^{-1} and consequently indicates that the chemical reaction control for the Cr(VI) reduction process is not likely, instead, an apparent catalysis of biofilm is more important.

Specific Cr(VI) reduction rates of 69–114 times and power production of 53–117 times as high as graphite plate cathodes [14], and 6.2–10.3 times and 5.2–12 times as graphite granules cathodes [23], respectively, were achieved in the present study in comparison with the values from the H-type MFCs. These specific Cr(VI) reduction rates were 3.6–6.1 times and 3.3–5.6 times, respectively, as high as those obtained from conventional aerobic and anaerobic Cr(VI) reduction processes [8]. These results allow us to better explore the potential of an efficient biocathode MFC for a quicker Cr(VI) reduction in comparison with conventional biological processes with simultaneously higher bioelectricity generation.

While Cr(VI) reduction rates and power generation were efficiently improved on the biocatalytic graphite fibers cathodes equipped with tubular MFCs, initial Cr(VI) concentrations, pH and temperature were proved to affect the performance of this system, illustrating the importance of system optimization for the present biocathode MFCs. In view of the fact that electron transfer from electrode surface to microorganisms was the most sluggish and difficult step, and consequently limiting the biocathode performance [55], more work needs to be done to clarify the electron transfer mechanisms using pure culture screened from the current biocathode system. For practical application and considerations, issues like retention of biomass and recovery of the reduced chromium in the scalable tubular biocathode MFC system need to be addressed. Complete removal of chromium may be achieved by intermittently pulling up the electrodes, and settling and removing the biomass from the cathode. The chromium can be then stripped off with a simple extractant such as sulfuric acid [56]. These subjects will need to be further investigated.

4. Conclusions

From this work, the following conclusions can be drawn:

(1) Carbon-based materials including graphite fibers, graphite felt and graphite granules equipped with tubular MFCs can efficiently improve both Cr(VI) reduction rates and bioelectricity production. Under the same ratio of C/A of 3, graphite fibers were superior to graphite felt or graphite granule. Specific Cr(VI) reduction rates and power production ranging from 12.4 mg g^{-1} VSS h^{-1} and 6.8 W m^{-3} (20 A m^{-3}) at C/A of 3 to 20.6 mg g^{-1} VSS h^{-1} and 15 W m^{-3} (48 A m^{-3}) at C/A

of 20 were achieved in biocatalyzed graphite fiber cathode MFCs.

(2) In comparison with pH 7.0, an acidic pH of 5.0 improved Cr(VI) reduction of 27.3% and power generation of 61.8% whereas an alkaline pH of 8.0 decreased Cr(VI) reduction of 21.2% and power generation of 6.0%. The products formed as dissolved and/or precipitated Cr(III) was highly pH dependent.

(3) Under a temperature of 22 °C and pH 7.0, Cr(VI) reduction followed the pseudo-first-order model. Elevating temperature from 22 to 50 °C increased Cr(VI) reduction with an increase in rate constant from 0.457 to 0.663 h^{-1} while electricity generation was decreased at a high temperature of 50 °C. The E_a obtained from this biocathode system was 10.6 kJ mol^{-1}.

Acknowledgments

The authors gratefully acknowledge financial support from the Natural Science Foundation of China (No. 21077017), Open Project of State Key Laboratory of Clean Energy Utilization (ZJUCEU2010001), Program for Changjiang Scholars and Innovative Research Team in University (IRT0813), and "Energy + X" (2008) key programme through Dalian University of Technology.

References

[1] E.M. Nkhalambayausi-chirwa, Y.T. Wang, Simultaneous chromium(VI) reduction and phenol degradation in a fixed-film coculture bioreactor: reactor performance, Water Res. 35 (2001) 1921–1932.
[2] F. Sevim, D. Demir, Investigation of reduction kinetics of $Cr_2O_7^{2-}$ in $FeSO_4$ solution, Chem. Eng. J. 143 (2008) 161–166.
[3] B. Geng, Z. Jin, T. Li, X. Qi, Kinetics of hexavalent chromium removal from water by chitosan-Fe^0 nanoparticles, Chemosphere 75 (2009) 825–830.
[4] Y. Chen, G. Gu, Preliminary studies on continuous chromium(VI) biological removal from wastewater by anaerobic–aerobic activated sludge process, Bioresour. Technol. 96 (2005) 1713–1721.
[5] A.H. Caravelli, L. Giannuzzi, N.E. Zaritzky, Reduction of hexavalent chromium by *Sphaerotilus natans* a filamentous micro-organism present in activated sludges, J. Hazard. Mater. 156 (2008) 214–222.
[6] A.A. Hasin, S.J. Gurman, L.M. Murphy, A. Perry, T.J. Smith, P.H.E. Gardiner, Remediation of chromium(VI) by a methane-oxidizing bacterium, Environ. Sci. Technol. 44 (2010) 400–405.
[7] W.A. Ahmad, Z.A. Zakaria, A.R. Khasim, M.A. Alias, S.M.H.S. Ismail, Pilot-scale removal of chromium from industrial wastewater using the ChromeBac™ system, Bioresour. Technol. 101 (2010) 4371–4378.
[8] P.E. Molokwane, K.C. Meli, E.M. Nkhalambayausi-Chirw, Chromium(VI) reduction in activated sludge bacteria exposed to high chromium loading: Brits culture (South Africa), Water Res. 42 (2008) 4538–4548.
[9] B.E. Logan, J.M. Regan, Microbial fuel cells: challenges and applications, Environ. Sci. Technol. 40 (2006) 5172–5180.
[10] Z. He, L.T. Angenent, Application of bacterial biocathodes in microbial fuel cells, Electroanalysis 18 (2006) 2009–2015.
[11] R.A. Rozendal, H.V.M. Hamelers, K. Rabaey, J. Keller, C.J.N. Buisman, Towards practical implementation of bioelectrochemical wastewater treatment, Trends Biotechnol. 26 (2008) 450–459.
[12] L. Huang, J.M. Regan, X. Quan, Electron transfer mechanisms, new applications, and performance of biocathode microbial fuel cells, Bioresour. Technol. 102 (2011) 316–323.
[13] D.R. Lovley, Powering microbes with electricity: direct electron transfer from electrodes to microbes, Environ. Microbiol. Rep. (2010), doi:10.1111/j.1758-2229.2010.00211.x.
[14] M Tandukar, S.J. Huber, T. Onodera, S.G. Pavlostathis, Biological chromium(VI) reduction in the cathode of a microbial fuel cell, Environ. Sci. Technol. 43 (2009) 8159–8165.
[15] B. Logan, S. Cheng, V. Watson, G. Estadt, Graphite fiber brush anodes for increased power production in air-cathode microbial fuel cells, Environ. Sci. Technol. 41 (2007) 3341–3346.
[16] P. Liang, X. Huang, M.Z. Fan, X.X. Cao, W. Cheng, Composition and distribution of internal resistance in three types of microbial fuel cells, Appl. Microbiol. Biotechnol. 77 (2007) 551–558.
[17] Y. Zuo, S. Cheng, D. Call, B.E. Logan, Tubular membrane cathodes for scalable power generation in microbial fuel cells, Environ. Sci. Technol. 41 (2007) 3347–3353.
[18] Y. Fan, H. Hu, H. Liu, Enhanced Coulombic efficiency and power density of air-cathode microbial fuel cells with an improved cell configuration, J. Power Sources 171 (2007) 348–354.
[19] B.E. Logan, Exoelectrogenic bacteria that power microbial fuel cells, Nat. Rev. Microbiol. 7 (2009) 375–381.
[20] M. Di Lorenzo, K. Scott, T.P. Curtis, I.M. Head, Effect of increasing anode surface area on the performance of a single chamber microbial fuel cell, Chem. Eng. J. 156 (2010) 40–48.
[21] P. Clauwaert, der H.D. Van, N. Boon, K. Verbeken, M. Verhaege, K. Rabaey, W. Verstraete, Open air biocathode enables effective electricity generation with microbial fuel cells, Environ. Sci. Technol. 41 (2007) 7564–7569.
[22] A. Aldrovandi, E. Marsili, L. Stante, P. Paganin, S. Tabacchioni, A. Giordano, Sustainable power production in a membrane-less and mediator-less synthetic wastewater microbial fuel cell, Bioresour. Technol. 100 (2009) 3252–3260.
[23] L. Huang, J. Chen, X. Quan, F. Yang, Enhancement of hexavalent chromium reduction and electricity production from a biocathode microbial fuel cell, Bioprocess Biosyst. Eng. 33 (2010) 937–975.
[24] K. Rabaey, P. Clauwaert, P. Aelterman, W. Verstraete, Tubular microbial fuel cells for efficient electricity generation, Environ. Sci. Technol. 39 (2005) 8077–8082.
[25] P. Clauwaert, K. Rabaey, P. Aelterman, L.D. Schamphelaire, T.H. Pham, P. Boeckx, N. Boon, W. Verstraete, Biological denitrification in microbial fuel cells, Environ. Sci. Technol. 41 (2007) 3354–3360.
[26] B. Virdis, K. Rabaey, Z. Yuan, J. Keller, Microbial fuel cells for simultaneous carbon and nitrogen removal, Water Res. 42 (2008) 3013–3024.
[27] S.J. You, N.Q. Ren, Q.L. Zhao, J.Y. Wang, F.L. Yang, Power generation and electrochemical analysis of biocathode microbial fuel cell using graphite fibre brush as cathode material, Fuel Cells 5 (2009) 588–596.
[28] H. Liu, S. Cheng, B.E. Logan, Power generation in fed-batch microbial fuel cells as a function of ionic strength, temperature, and reactor configuration, Environ. Sci. Technol. 39 (2005) 5488–5493.
[29] H. Moon, I.S. Chang, B.H. Kim, Continuous electricity generation from artificial wastewater using a mediator-less microbial fuel cell, Bioresour. Technol. 97 (2006) 621–627.
[30] Y. Feng, X. Wang, B.E. Logan, H. Lee, Brewery wastewater treatment using air-cathode microbial fuel cells, Appl. Microbiol. Biotechnol. 78 (2008) 873–880.
[31] Z. He, Y. Huang, A.K. Manohar, F. Mansfeld, Effect of electrolyte pH on the rate of the anodic and cathodic reactions in an air-cathode microbial fuel cell, Bioelectrochemistry 74 (2008) 78–82.
[32] G.S. Jadhava, M.M. Ghangrekar, Performance of microbial fuel cell subjected to variation in pH, temperature, external load and substrate concentration, Bioresour. Technol. 100 (2009) 717–723.
[33] Y. Ahn, B.E. Logan, Effectiveness of domestic wastewater treatment using microbial fuel cells at ambient and mesophilic temperatures, Bioresour. Technol. 101 (2010) 469–475.
[34] P. Clauwaert, J. Desloover, C. Shea, R. Nerenberg, N. Boon, W. Verstraete, Enhanced nitrogen removal in bio-electrochemical systems by pH control, Biotechnol. Lett. 31 (2009) 1537–1543.
[35] G. Wang, L. Huang, Y. Zhang, Cathodic reduction of hexavalent chromium [Cr(VI)] coupled with electricity generation in microbial fuel cells, Biotechnol. Lett. 30 (2008) 1959–1966.
[36] P. Aelterman, S. Freguia, J. Keller, W. Verstraete, K. Rabaey, The anode potential regulates bacterial activity in microbial fuel cells, Appl. Microbiol. Biotechnol. 78 (2008) 409–418.
[37] S.B. Velasquez-Orta, T.P. Curtis, B.E. Logan, Energy from algae using microbial fuel cells, Biotechnol. Bioeng. 103 (2009) 1068–1076.
[38] State Environmental Protection Administration, The Water and Wastewater Monitoring Methods, 4th ed., China Environmental Science Press, Beijing, 2002.
[39] X. Cao, X. Huang, P. Liang, N. Boon, M. Fan, L. Zhang, X. Zhang, A completely anoxic microbial fuel cell using a photo-biocathode for cathodic carbon dioxide reduction, Energy Environ. Sci. 2 (2009) 498–501.
[40] K. Rabaey, S.T. Read, P. Clauwaert, S. Freguia, P.L. Bond, L.L. Blackall, J. Keller, Cathodic oxygen reduction catalyzed by bacteria in microbial fuel cells, ISME J. 2 (2008) 519–527.
[41] X. Yang, H. Beyenal, G. Harkin, Z. Lewandowski, Quantifying biofilm structure using image analysis, J. Microbiol. Methods 39 (2000) 109–119.
[42] K. Kawai, M. Urano, S. Ebisu, Effect of surface roughness of porcelain on adhesion of bacteria and their synthesizing glucans, J. Prosthet. Dent. 83 (2000) 664–667.
[43] M. Quirynen, C.M. Bollen, The influence of surface roughness and surface-free energy on supra- and subgingival plaque formation in Man: a review of the literature, J. Clin. Periodontol. 22 (1995) 1–14.
[44] H. Tang, T. Cao, A. Wang, X. Liang, S.O. Salley, J.P. McAllister, Ng.K.Y. Simon, Effect of surface modification of silicone on *Staphylococcus epidermidis* adhesion and colonization, J. Biomed. Mater. Res. A 80A (2007) 885–894.
[45] T.A. Nguyen, Y. Lu, X. Yang, X. Shi, Carbon and steel surfaces modified by *Leptothrix discophora* SP-6: characterization and implications, Environ. Sci. Technol. 41 (2007) 7987–7996.
[46] C. Dumas, R. Basseguy, A. Bergel, Microbial electrocatalysis with *Geobacter sulfurreducens* biofilm on stainless steel cathodes, Electrochim. Acta 53 (2008) 2494–2500.
[47] K.P. Nevin, H. Richter, S.F. Covalla, J.P. Johnson, T.L. Woodard, A.L. Orloff, H. Jia, M. Zhang, D.R. Lovley, Power output and columbic efficiencies from biofilms of *Geobacter sulfurreducens* comparable to mixed community microbial fuel cells, Environ. Microbiol. 10 (2008) 2505–2514.
[48] M. Behera, P.S. Jana, J.M.M. Ghangrekar, Performance evaluation of low cost microbial fuel cell fabricated using earthen pot with biotic and abiotic cathode, Bioresour. Technol. 101 (2010) 1183–1189.
[49] R.A. Rozendal, H.V.M. Hamelers, C.J.N. Buisman, Effects of membrane cation transport on pH and microbial fuel cell performance, Environ. Sci. Technol. 40 (2006) 5206–5211.

[50] M.M. Walczak, D.A. Dryer, D.D. Jacobson, M.G. Foss, N.T. Flynn, pH-dependent redox couple: illustrating the Nernst equation using cyclic voltammetry, Environ. Sci. Technol. 74 (1997) 1195–1197.
[51] Q.S. Luo, H. Wang, X.H. Zhang, Y. Qian, Effect of direct electric current on the cell surface properties of phenol-degrading bacteria, Appl. Environ. Microbiol. 71 (2005) 423–427.
[52] J.P. Busalmen, S.R. De Sanchez, Electrochemical polarization-induced changes in the growth of individual cells and biofilms of *Pseudomonas fluorescens* (ATCC 17552), Appl. Environ. Microbiol. 71 (2005) 6235–6240.
[53] M.S. Elovitz, W. Fish, Redox interactions of Cr(VI) and substituted phenols: products and mechanisms, Environ. Sci. Technol. 29 (1995) 1933–1943.
[54] P.R. Wittbrodt, C.D. Palmer, Reduction of Cr(VI) in the presence of excess soil fulvic acid, Environ. Sci. Technol. 29 (1995) 255–263.
[55] A.E. Franks, K.P. Nevin, Microbial fuel cells: a current review, Energies 3 (2010) 899–919.
[56] S.B. Shen, R.D. Tyagi, R.Y. Surampalli, J.F. Blais, Laboratory pilot test of chromium(III) isolation from acid extract of tannery sludge, Pract. Periodical Haz. Toxic Radioactive Waste Manag. 7 (2003) 59–65.